Ultrasound in Med. & Biol. Vol. 15, No. 1, pp. 21–28, 1989
Printed in the U.S.A.

0301-5629/89 $3.00 + .00

●*Original Contribution*

ASSESSMENT OF ULTRASONIC COMPUTED TOMOGRAPHY IN SYMPTOMATIC BREAST PATIENTS BY DISCRIMINANT ANALYSIS

ANN L. SCHERZINGER,† ROBERT A. BELGAM,† PAUL L. CARSON,‡
CHARLES R. MEYER,† JEFFREY V. SUTHERLAND,† FRED L. BOOKSTEIN‡
and TERRY M. SILVER‡

†Department of Radiology, University of Colorado, School of Medicine, Denver, CO 80262,
‡Department of Radiology, University of Michigan Medical Center, Ann Arbor, MI 48109

(*Received* 6 *March* 1986; *in final form* 24 *May* 1988)

Abstract—From 95 subjects imaged with both speed of sound and attenuation ultrasonic computed tomography (UCT), quantitative analyses are presented on 40 cases where unequivocal correlating clinical diagnoses are available. Using four attenuation and speed of sound parameters from different regions of interest in the breast, a linear discriminator detects cancer with approximately 90% sensitivity and specificity. Increased confidence in the predictive power of this small study is given by a modern test of predictive power (jackknifing) and by the fact that diagnostic discrimination remains as high as 85% when only two parameters are employed—attenuation and speed of sound in the lesion minus those values in the remaining central mammary tissues. Speed of sound images appear particularly useful in older, fatty breasts where pulse echo ultrasound is particularly lacking. While UCT in the form studied here is not likely to receive wide clinical acceptance in the near future, a combined UCT/pulse echo system might find wide clinical utility if it can be sufficiently convenient and inexpensive.

Key Words: **Breast cancer diagnosis, Ultrasound imaging, Tissue characterization, Computed tomography.**

INTRODUCTION

Currently the most widely used ultrasonic breast imaging method is the conventional pulse echo scan. It is thought that the addition of quantitative, tissue-specific information not provided by pulse echo imaging has a high probability of increasing the diagnostic accuracy over that achievable with only pulse echo techniques. Several researchers have demonstrated that quantitative images of acoustic speed and semiquantitative images of acoustic attenuation of tissues can be obtained using ultrasonic computed tomography (UCT) (Greenleaf et al., 1974; Glover, 1977; Greenleaf et al., 1978; Carson et al., 1978). Attenuation measures are referred to as only semi-quantitative because attenuation measures suffer from edge enhancement and suppression of contrast in homogeneous regions due to refraction, reflection, and multiple path splitting of the ultrasound beam by tissue interfaces encountered at oblique angles (Klepper et al., 1977; Kak and Dines, 1978; Johnson et al., 1975, Mueller et al., 1979; Meyer et al., 1982; Crawford and Kak, 1982; Pan and Liu, 1981; Chenevert et al., 1983). Comparisons of pulse echo and UCT images have also been reported (Carson et al., 1981; Koch et al., 1983). From the studies of 40 patients presented below we have previously employed simple visually implementable interpretive criteria as described in a related paper (Carson et al., 1988) and have evaluated a set of quantitative, speed of sound and attenuation criteria which could be implemented reasonably well visually (Carson et al., 1983). In this paper quantitative discriminant analysis on images of these patients is presented to detect and evaluate relevant quantitative diagnostic criteria. Analysis of a similar group of patients was presented by Greenleaf et al. (1983), and Schreiman et al. (1984).

Address reprint requests to: Paul L. Carson, Ph.D., Radiology Physics and Engineering, University of Michigan Hospitals, 1500 E. Medical Center Drive, Ann Arbor, MI 48109-0553, (313) 763-5884.

METHODS

Subject population and tissue classifications

The patient is imaged while lying prone on an examination table with one breast immersed in a water tank via a circular aperture in the table. Pulse echo (Carson et al., 1981) and UCT speed of sound

and attenuation coronal images, are generated by a translate-rotate motion of opposing 3.5 MHz transducers in a water tank (Carson et al., 1979). Speed and attenuation images are displayed on a CRT where region of interest software allows the calculation of mean propagation speeds and attenuation coefficients, with their variances, for selected areas of interest. Pulse echo images are displayed on an analog scan converter and photographed for analysis. In all the images, high values of attenuation and speed of sound were depicted as white on a dark background.

Included in this study are examinations from 40 cases, 36 *in vivo* and 4 *in vitro*. Subjects chosen exhibited clinically palpable or mammographically detected areas of concern or "lesions" in which both attenuation and speed of sound images were technically acceptable. Additional details of the imaging methods and subject population are given in (Carson et al., 1988).

A majority of breast studies exhibited P2 patterns (Wolfe, 1967) mammographically. The distribution of pathologies included 6 normal breasts, 10 unclassified benign lesions, 8 cysts, 4 fibroadenomas, and 12 carcinomas (8 *in vivo*, 4 *in vitro*). All lesions were larger than 1 cm in diameter and were easily palpable. The pathology group labelled "unclassified benign" included non-malignant lesions and regional disease processes such as fibrocystic disease, fibrosis, adenosis, sclerosing adenosis, lobular and ductal dysplasia. All cancers were infiltrating ductal. Diagnosis was confirmed by biopsy in 29 cases, by mammography in 10 (benign lesions) and by clinical evaluation in 1 case (normal tissue). Recent followup on 10 of these 11 cases not confirmed by biopsy has shown no evidence of cancer, nor change in the initial diagnosis of at least five years ago.

Ten regions were analyzed in the images of the 40 patients included in the analysis, 7 in the suspect

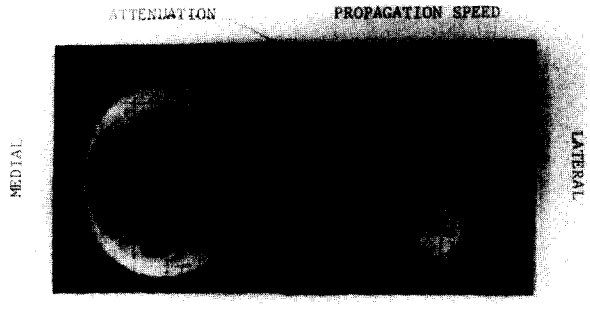

Fig. 1. Attenuation and speed of sound UCT images of normal left breast of a young woman. A coronal plane is shown, as if facing the patient. Regions used for quantitative analysis are shown.

Table 1. Summary of regions included in the study.

Region	Description
	Involved breast:
1	Lesion—center 20 pixels
2	Lesion—full width at half maximum (FWHM) border
3	Lesion—around border on attenuation image
4	Homogeneous fat tissue (1–4 cm^2)
5	Highest speed of sound, nonlesion tissue of ≥ 1 cm^2
6	Breast parenchyma—excluding lesion
7	Entire breast
	Uninvolved breast:
8	Highest speed of sound tissue (>1 cm^2)
9	Breast parenchyma
10	Entire Breast

breast and 3 in an image at a comparable level in the opposite breast. In Fig. 1, these regions are illustrated on the UCT images at one level through a palpable firm area in the breast of a 28-year-old. For each patient analyzed, a palpable or mammographically suspect region is defined as the lesion, even though it may be proven normal or benign histologically. In this patient a palpable tissue of concern was noted in the upper outer quadrant (region 3) and was later diagnosed to be normal fibrous breast tissue. The UCT attenuation image shows the mass clearly as fibrous tissue associated with a Cooper's ligament.

Disease processes are commonly indicated by the presence of tissue exhibiting a higher than normal average speed of sound. Thus, when there is doubt, the lesion is chosen as that region with high speed of sound which best correlates in location and size with that seen on mammography, by palpation, and/or by direct correlation with surgical and histological results. Possible exceptions to this rule would be where the diagnosis indicates a fatty lesion. Often, the borders of the lesions are easily observed on the attenuation and/or pulse echo image and lesions appear larger in size on these images. Whenever possible the lesion borders and ROI's were defined by the attenuation image and then superimposed on the corresponding area in the velocity image.

As summarized in Table 1, regions 1–3 describe the lesion. The lesion border is defined in region 2 as the locus of CT numbers having a value equal to the mean of the lesion background and the lesion maximum speed of sound value. This full width at half maximum (FWHM) definition is used to provide a consistent means of defining lesion edges, even when they are not visible on the attenuation or pulse echo images. On the patient in Fig. 1, subcutaneous fat tissue lobules are readily seen as low attenuation and low speed of sound regions (region 4), separated by ligaments and lying adjacent to the highly attenuating skin border. The appearance of high attenuation at

the skin results in part from refraction and reflection of the beam at the water-tissue interface. Consistent with earlier studies (Kossoff et al., 1973), average values of UCT parameters measured for the entire breast decrease with age as breast parenchyma is replaced by adipose tissue. For the young, dense breast of Fig. 1, the measured speed of sound and attenuation number for normal parenchyma (region 6) are 1549 ± 28 m/s and 2.7 ± 1.1 AU (attenuation units), respectively, while those for the entire breast (region 7) are 1522 ± 38 m/s and 3.4 AU. The average values for the speed of sound and attenuation number of region 7 in the older [greater than 50 years old] breasts examined were 1475 m/s and 2.2 AU at an effective frequency of approximately 3.1 MHz.

The attenuation number in attenuation units, AU, is numerically equal to the signal attenuation measured, in decibels per centimeter. However, the reconstructed attenuation values for a given tissue are very dependent on the particular transducer configuration employed, on details of the signal processing and, most importantly, on the properties of surrounding tissues. For this reason we wish to avoid strong identification and quantitative numbers with specific tissues, while still making known the limited information available from this particular transmission imaging system.

Discriminant analysis

Linear discriminant analysis is a conventional statistical procedure for testing the extent to which groups such as various classes of lesions can be discriminated on the basis of their quantitative characteristics (Lachenbruch, 1975; McNeil and Hanley, 1981; Nie et al., 1975). The F-ratio, familiarly used in the conventional statistical test for separation of two group means on a single variable score, is a ratio of two variances. The numerator is the variance due to the scatter of group means; the denominator is the variance due to the scatter of the scores about their means within each group.

Suppose that many variables, such as attenuation (atten) and speed of sound (sos), for each of our 10 breast regions, have been measured on subjects in two or more groups. Consider all the linear scores that can be constructed out of these raw measures, *i.e.*, all the linear functions

$$c_{a1}\text{atten}_1 + c_{s1}\text{sos}_1 + \cdots + c_{a10}\text{atten}_{10} + c_{s10}\text{sos}_{10}$$

constructed from any values of the twenty coefficients $c_{a1} \cdots c_{a10}, c_{s1} \cdots c_{s10}$. These functions represent all possible linear combinations of absolute levels and contrasts by which we might characterize the lesions. For instance, the score $c_{a1} = 1$, $c_{a7} = -1$, with all other c's equal to zero, represents a contrast, $\text{atten}_1 - \text{atten}_7$. That contrast is, the elevation of the lesion attenuation above that of the surrounding tissue.

It is useful to compute the one of those linear scores which yields the largest F-ratio for a test of group separation. This score would yield the largest predominance of real group difference (signal) to within-group variance (noise) in the context of group discrimination. Once such a function $c_{a1}\text{atten}_1 + \cdots + c_{s10}\text{sos}_{10}$ is available, it may be used to classify each lesion into one of the two or more groups according to its score. In effect, it is assigned to the group whose centroid is closest to the lesion score after correction for correlation among the variables. Sometimes this assignment takes cognizance of prior probabilities of group membership, so that, for instance, a group with 60% of the sample is assigned 60% of the specimens. Or different misclassifications may be ascribed different costs: for instance, the cost of a false negative for cancer may be set to many times the cost of a false positive. Because the group membership fractions in this analysis are an arbitrary consequence of the sample design, we did not correct the classification function in the first of these ways, although the correction could be justified and increased weighting of false negatives would increase the sensitivity significantly.

This style of analysis is exemplified in Fig. 2, which demonstrates the discrimination of two groups

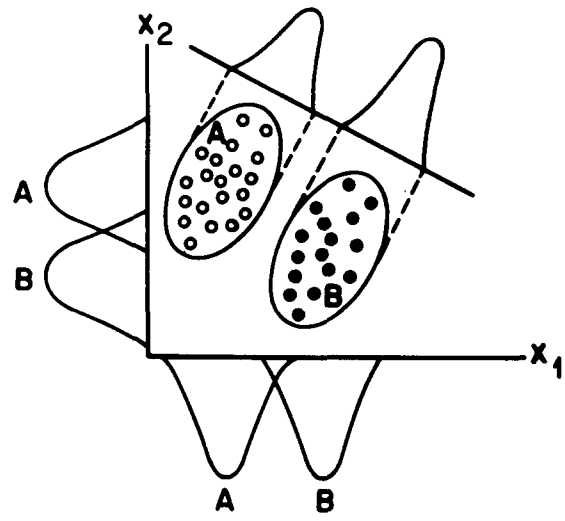

Fig. 2. Shown on the orthogonal axes are plots of the distributions of groups A and B in variables X1 and X2. Both features X1 and X2 show a considerable overlap between groups, but with the combination of X1 and X2 (sloping line), the groups of patients are completely separated.

by a linear combination of the two variables shown. It is evident how the groups overlap much less in projection along the line indicated than they overlap on either of the original two variables.

In the presence of more than two groups, one arrives at more than one discriminant function. The first is the one just characterized, the score yielding the best F-ratio of all scores. The second is the score yielding the best F-ratio of all scores that share no information (*i.e.*, are uncorrelated) with the first score, and so on. The discrimination of K groups requires, in general, $K - 1$ of these functions.

Accuracy estimates and jackknifing. The statistical power of discriminant analysis can be tested by way of the F-ratios used to compute the scores. The logic of this is the logic usual in statistical significance testing, the check of whether the null hypothesis of no group differences can be reflected. Such a test is not suited to the clinical needs here, as it is a function of sample size. We are interested instead in the classification accuracy (and sensitivity, and specificity) yielded by the decision rule chosen. Specifically, an estimate is required for the probability that a new specimen, not among those needed for computing the F-ratio that is being optimized, will be classified correctly. This test is simulated by a procedure called jackknifing. It is implemented by running the same discriminant analysis N times, where N is the number of available cases. In each run, one of the N specimens is omitted from the computation of the F-ratio, and then classified based on the discriminant score derived from the other $N - 1$ specimens.

Reduction of variables. A linear discriminant score has one coefficient for each variable, a total of 20 coefficients for the 10 regions of interest recorded in this study. It is very difficult to interpret such a long list of numbers. Most computer packages come to our aid in this matter by discriminating stepwise. That is, they try combinations of one, two, three, . . . variables at a time, until additional variables add no more power to the F-test. On our data in which lesions' classes are combined into three groups (Table 2), this procedure resulted in the two discriminant functions of Table 3, based on four most helpful variables as listed. For expository purposes it is useful to reduce this still further, to a qualitative verbal formulation. Discriminant function #2 can be viewed as the approximate sum of two contrasts: lesion speed of sound relative to that in the normal parenchyma, and lesion attenuation relative to whole breast attenuation. Function #1 can be summarized as the approximate difference of those two contrasts. (In this summary we are ignoring differences in the ratios of the coefficients in the two functions.) This simplification may be exploited to pose a new problem: the optimal discrimination of the three groups by these two arbitrary (but nearly optimal) contrasts alone. These contrasts are of interest because they are very simple to measure from single images, and easy to report. The analysis of the discrimination based on these two scores occupies Fig. 3 and the right-hand side of the Table 4 below.

Table 2. Group membership for discriminant analysis.

No. of groups	Group division
3	Cancer, cystic, noncancer solid
4	Cancer, cystic, benign solid, normal
5	Cancer, fibroadenoma, benign solid, cystic, normal

Table 3. Weighting coefficients c_{s3}, c_{s6}, c_{a2}, c_{a7} for three group analysis.

	Unstandardized weighting coefficient	
Variable	Function 1	Function 2
Lesion speed (region 3)	0.02085	−0.03229
Normal tissue speed (region 6)	−0.04313	0.03352
Lesion attenuation (region 2)	−1.085	−1.082
Entire breast attenuation (region 7)	0.586	+0.894
Constant	33.54	−0.56

RESULTS

In Table 5 the measured speed and relative attenuation values are compared with those of Greenleaf and Bahn (1981) and with the speed values calculated from Glover's (1977) UCT numbers assuming a speed of sound in water of 1518 m/s. Large standard deviations and only small differences in the average speed of sound and attenuation between various tissues are noted. It appears that classification of breast tissues is more complex than a simple comparison of acoustic parameters from a single tissue in the breast with average values in a table. The following paragraphs describe the results of the discriminant analysis performed to select which combination of acoustic variables is most useful for the classification of breast pathologies and to provide an indication of how well a classification of breast pathologies can be performed with UCT measurements.

For the most part the linear discrimination of the sample is reported according to three groups: cysts, other non-malignant lesions, and cancer. (A few analyses use four or five groups as listed in Table 2.)

In the three group analysis, a stepwise procedure

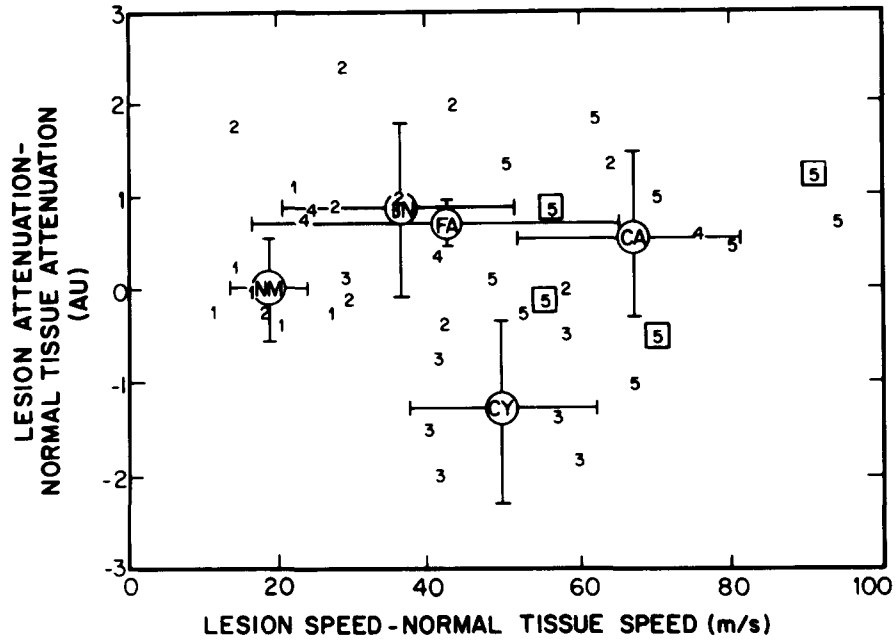

Fig. 3. A plot of tissue characteristics of each of the 40 lesions in terms of intuitively meaningful referenced variables. That is, the variables are composed of the speed and attenuation of sound in the lesions subtracted, respectively, from the speed and attenuation of the remaining central mammary tissue. The five lesions of groups are shown with ellipses indicating one standard deviation of the group data points. Lesion groups and their representations are: normal-1, unclassified benign-2, cyst-3, fibroadenoma-4, cancer-5. *In vitro* cancers are outlined in a square. The various lesion groups would not be separated and clustered as well if plotted only in terms of the lesion speed and attenuation or in terms of the lesion speed and attenuation weighted by patient age. (Cancer in a fatty breast appears, perhaps artifactually, to have a lower speed of sound. This probably explains the reduced speed of sound observed in cancer as a function of age.)

according to the usual criteria terminated after the entry of four variables. The weighting coefficients c_{a2}, c_{s3}, c_{s6}, c_{a7} in the principal (three-group) analysis are listed in Table 3; their linear combinations are found to be the most useful linear discriminators. As in Table 3, the coefficients of the two speed of sound variables are always of opposite sign, indicating a contrast; likewise the coefficients of the two regional attenuations are always of opposite sign. In these forty patients none of the variables for the opposite breast (regions 8, 9, and 10) are particularly useful in discriminating the lesion type. Recall, however, that the role of asymmetry in locating the lesion is not taken into account in this statistical analysis.

Table 4. Classification accuracy, sensitivity and specificityof discriminant functions obtained.

No. of groups	Four variables			Two relative variables†		
	Accrc	Senstv	Specf	Accrc	Senstv	Specf
3	90	92	93	85	83	89
4	85	92	93	73	67	86
5	78	92	93	63	75	86
3‡	83	83	86	78	67	89

† The difference in lesion and normal tissue attenuation (R2–R6) and speed (R2–R6) (see text).

‡ Using iterative (jackknifing) method (see text).

Accrc = accuracy; Senstv = sensitivity; Specf = specificity; List: 16.

The contrast of speed of sound parameters is consistent with that noted from qualitative analysis of the images. It now appears that we may think of attenuation as a contrast in the same way. By arbitrarily setting the two coefficients, we can generate a scatter as in Fig. 3 of the forty cases upon axes which are easily described verbally: differences in speed of sound and in attenuation between region 2 and region 6. In Fig. 3, the groups are identified by number as listed in the caption. A cross indicating the standard deviations of these scores within group is plotted at each group centroid. From this scatter we note the need for two discriminant functions to distinguish the three groups. Malignant lesions are distinguished by their higher relative speed of sound. *In vitro* lesions fall randomly within the range of the *in vivo* cancerous lesions. Cystic structures, with an intermediate speed of sound, are distinguished by their low relative attenuation. Most solid non-malignant lesions are distinguished by their low speed of sound, however,

Table 5. Comparison of ultrasound speed and relative attenuation in selected breast tissues *in vivo*.

Tissue	Rel. atten. This work Re Ref 6 (R6)† (AU)*	Rel. atten. Greenleaf	Speed of sound This Work Center Reg† (R1)	Speed of sound This Work 1/2 Max Reg‡ (R2)	Speed of sound Greenleaf	Speed of sound Glover
Cancer gp 1	0.5 ± 0.8	15 ± 80%	1550 ± 35	1530 ± 23	1480–1545	1579–1601
Cancer gp 2		8–30%			1570–1580	
Fibroadenoma	0.7 ± 0.2	5–60%	1584 ± 27	1565 ± 17	1540–1575	1548–1561
Cyst	−1.3 ± 1.0		1568 ± 40	1548 ± 30		1518–1520
Benign solid	0.9 ± 1.0		1561 ± 32	1545 ± 31		
Fibrocystic		0.8%			1470–1585	1548–1564
Normal "mass"	0.2 ± 0.6		1553 ± 35	1538 ± 22		
Highest speed normal tissue						
Involved breast (R5)	0.3 ± 1.2			1522 ± 36		
Parenchyma—Normal tissue						
Involved breast (R6)	=0	20–60%		1493 ± 34	1445–1500	1530–1609
Contralateral (R9)	0.2 ± 1.0			1498 ± 38		
Entire breast						
Suspect (R7)	0.5 ± 1.0			1483 ± 30		
Contralateral	0.5 ± 0.9			1479 ± 32		
Fat-subq. and older central‡	−1.5 ± 1.0	0–60%		1451 ± 36	1350–1430	1427

* See text for attenuation units, AU.
† R = region (see Table 1).
‡ Subcutaneous and older, centrally located fat tissue.

notice that the four firbroadenomas cannot be correctly classified using this pair of classifying variables. Schreiman et al. (1984) reported four categories for malignant lesions based on a similar pair of classifying variables. Our results are consistent with their first three categories which classify malignant lesions as having high relative speed of sound with variable relative attenuation (low to high). No cancers in our group were found to fall into the fourth category: low relative speed of sound with high relative attenuation.

The two discriminant functions of Table 3 separate the forty lesions into three groups with an overall accuracy of 90% as summarized in Table 4. Regarding the detection of cancer, the sensitivity is 92% and the specificity 93%. Figure 4 shows the nature of the misclassifications in the scatter of these two variables. One *in vitro* (infiltrating ductal carcinoma, plotted with the symbol "5" is classified as a solid benign lesion (group 2), but with a 0.32 probability of being in group 5. This was a young 33 year old with relatively low speed of sound contrast in the lesion, 1523 m/s, relative to that of normal tissue, 1497 m/s. Two solid benign lesions ("2") (one fibrocystic lump, one fibroadenoma) were classified as cancers (group 5); and one cyst ("3"), was misclassified as a solid benign lesion (group 2). Three of the four misdiagnoses lie near the classification lines in this plane projection. All cancers were infiltrating ductal with some exhibiting other forms of carcinoma as well [papillary, (2), adenocarcinoma (1), lobular (3)]. A breakdown of UCT parameters by secondary carcinoma type showed no consistent patterns. (When the solid benign lesions were subdivided, so as to classify the subjects into four or five groups, overall accuracy diminished to 85% or 78%. But the cancers were still classified with the same sensitivity and specificity; the loss of accuracy was entirely between classes within the category of solid benign lesions.) When the three-group classification was repeated using the two relative variables rather than the four separate measures detected by the stepwise algorithm, overall accuracy decreased to 85%, sensitivity for cancer to 83%, and specificity for cancer to 89%. The corresponding scatter (Fig. 3) shows that in this space the group centroids lie close together, with more overlap, than they do in Fig. 4, which is, of course, optimized for that separation. The work of Schreiman et al. (1984) indicated a comparable sensitivity of 82.5%, yet a much lower specificity of 60.5% due to a large number of false positives.

None of these accuracy figures correspond to what we would expect if we extended our procedure to classify unknown samples. The jackknifed analysis corresponding to the discriminant functions of Table 3 showed an overall prospective accuracy of 83% instead of 90%, with a sensitivity for cancer detection of 83% and a specificity of 86%. In the jackknifed classification based on the remaining 39 cases, two cancers

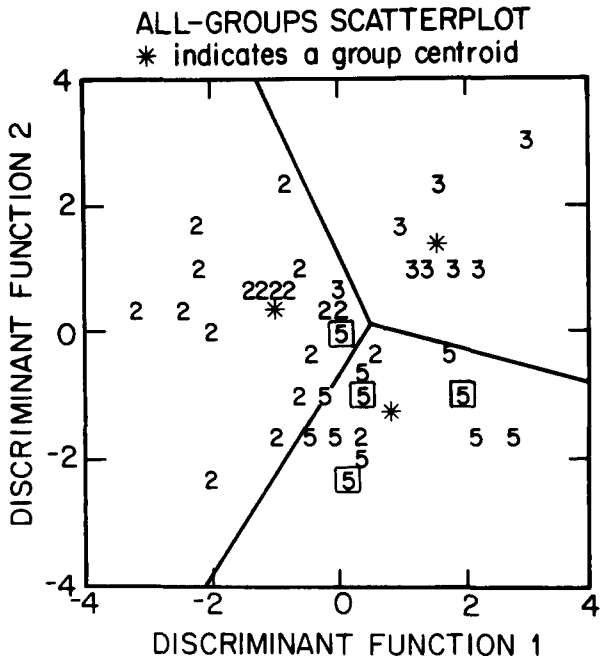

Fig. 4. Plot of lesion characteristics of three groups in terms of two discriminant functions comprised of linear combinations of the four most discriminating variables. Group representation are: 2-noncancer solid, 3-cystic, 5-cancer, *-group centroid.

were classified as solid benign lesion; one of eight cysts was also so classified, three of sixteen benign solid masses, and one of four fibroadenomas, were classified as cancers. As before, discrimination based on the two relative variables, or discrimination into four or five classes, resulted in decreased accuracy.

DISCUSSION AND CONCLUSION

Results of this quantitative analysis of UCT breast imaging of 40 patients are encouraging. Discriminant analysis of the images indicates that the important variables for lesion characterization are the high speed of sound of malignant tissue when compared to normal tissues of the same breast and the comparison of lesion attenuation and that of the entire breast. With these criteria alone, a sensitivity and specificity to cancer versus solid benign masses and cysts of approximately 83 and 86% is obtained. Similar variables plus breast asymmetry were seen to be important in the visually oriented analysis of images (Carson et al., 1988). But that evaluation utilized only the sign of the differences of speeds of sound, rather than the magnitude of linear combinations of variables.

Further division of the benign lesions into more groups decreased overall accuracy in the UCT study but not sensitivity or specificity defined on the basis of separating benign from malignant conditions. Lower false negative rates are obtainable if the discriminant analysis is coded to weight the risk and cost of false negatives higher than those of false positives. Contrary to Glover's (1977) suggestion from earlier studies, the speed of sound of the entire involved breast (region 7) does not appear to be a useful discriminator of cancer.

In discriminant analyses of future UCT studies with larger data bases, variables describing the contralateral breast may improve the discrimination. The low significance in this study of information on the contralateral breast may have resulted from the lack of that information in four of twelve malignant lesions. Lesion size and location are other variables which, although not included in this study, are of possible significance due to their potential influence on the ultrasonic characteristics of lesions.

There was some bias upward in lesion detection in the course of this study, but we are hopeful that the bias was relatively small. Where several regions of high speed of sound were present in an image, the one best matching the external evidence (mammography, palpation, etc.) was selected. Often a distinctive attenuation border pointed toward selection of that same lesion. The success of UCT in this study also is indicative of the largely older patient population imaged. In a speed of sound image, a carcinoma with a high speed of sound is highly visible in a fatty breast with generally low speed of sound. Cases missed were mainly those involving cancer in young dense breasts, yet that is where mammography is also most lacking and a good supplement is required. Limited experience with the technique, based on a relatively small number of patients over a protracted period, provided a small downward bias in the reported lesion discrimination.

While the statistics on lesion discrimination are good, it is not clear that the technique as studied here is yet adequate to assume a major role in breast cancer detection and diagnosis. In the radiographically dense breast, pulse echo ultrasound has proven useful in many investigators' experience. UCT adds additional information to that obtainable with pulse echo ultrasound. If major improvements in UCT information content do not appear to be forthcoming in the next few years it may prove worthwhile to construct a convenient, fast UCT/pulse echo scanner with the then existing technology. This would allow the necessary second and third phase clinical trials, to assess the true value of combined UCT and pulse echo ultrasound in patient management. Such studies might well prove positive if the system were sufficiently convenient in patient scanning and interpretation and of sufficiently low cost.

Throughout this study we have noted that the speed of sound measurements are relatively precise representations of tissue properties offering relative independence from the amount and properties of surrounding tissues, notwithstanding the 1% artefactural decrease in the measured speed of sound expected for cancer in a fatty breast. This is due to a time walk artefact from 5 dB average attenuation at the tumor border (Lambert, 1979; Koch et al., 1983). The time walk speed of sound artefact can be almost eliminated by various methods of pulse arrival time detection (Chenevert et al., 1984). However, the attenuation images implemented in patient studies to-date are only semiquantitative. They bear edge enhancement artifacts arising from diffraction, reflection, and path splitting of the ultrasound beam. In some cases the edge enhancement feature offers some advantage in helping to demarcate boundaries and regions of interest. While the relative attenuation values from a tissue region in the images are determined in part by properties of surrounding tissues, the observed attenuation is reflective enough of the bulk tissue properties to be useful in solid/cyst differentiation in quantitative as well as visual analyses. Many studies of alternative detection and signal processing have been performed. They are reviewed in recent publications (Klepper et al., 1977; Kak and Dines, 1978; Schmitt et al., 1984; Fitting et al., 1984) which indicate clear improvements in quantitative accuracy of attenuation imaging are achievable in practical systems.

Acknowledgment—This work was supported in part by PHS grant number 2 R01 CA31857 awarded by the National Cancer Institute DHHS.

REFERENCES

Carson, P. L.; Dick, D. E.; Thieme, G. A.; et al. Initial investigation of computed tomography for breast cancer imaging with focused ultrasound beams. Ultras. Med. 4:1319–1322; 1978.

Carson, P. L.; Meyer, C. R.; Scherzinger, A. L.; Oughton, T. V. Breast imaging in coronal planes with simultaneous pulse echo and transmission ultrasound. Science 214:1141–1143; 1981.

Carson, P. L.; Scherzinger, A. L.; Bland, P. H.; Meyer, C. R.; Schmitt, R. M.; Chenevert, T. L.; Bookstein, F. L.; Bylski, D. I.; Silver, T. M. Ultrasonic computed tomography instrumentation and human studies. In: Jellins, J.; Kobayashi, T., eds. Ultrasonic imaging of the breast. Chichester: Wiley; 1983:187–199.

Carson, P. L.; Scherzinger, A. L.; Meyer, C. R.; Moore, G. E.; Jobe, W.; Samuels, B. Lesion detectability in ultrasonic computed tomography in symptomatic breast patients. Invest. Radiol. 23:421–427; 1988.

Carson, P. L.; Scherzinger, A. L.; Oughton, T. V.; et al. Progress in ultrasound computed tomography (CT) of the breast. In: Hendee, W. R.; Gray, J. E., eds. Proc. SPIE Vol. 173. Bellingham, WA: Soc. Photo-optical Instrum. Engineers; 1979:372–381.

Chenevert, T. L.; Meyer, C. R.; Bland, P. H.; Bakshi, C. C.; Carson, P. L. Aperture diffraction theory applied to ultrasonic attenuation imaging. J. Acoust. Soc. Am. 74:1232–1238; 1983.

Chenevert, T. L.; Bylski, D. I.; Carson, P. L.; Meyer, C. R.; Schmitt, R. M.; Bland, P. H.; Adler, D. L. Ultrasonic computed tomography of the breast. Radiology 152:155–159; 1984.

Crawford, C. R.; Kak, A. C. Multipath artifact corrections in ultrasonic transmission tomography. Ultras. Imag. 4:234–266; 1982.

Fitting, D.; Schmitt, R. M.; Grounds, P.; Hansel, G.; Carson, P. L. Development of two-dimensional PVDF arrays for transmission computed tomography of attenuation. In: McAvoy, B. R., ed. 1984 ultras. symp., procs. IEEE cat. no. 84CH2112-1. New York: IEEE; 1984:794–797.

Glover, G. H. Computerized time-of-flight ultrasonic tomography for breast examination. Ultras. Med. Biol. 3:117–128; 1977.

Greenleaf, J. F.; Bahn, R. C. Clinical imaging with transmissive ultrasonic computerized tomography. IEEE Trans. Biomed. Eng. BME-28:177–185; 1981.

Greenleaf, J. F.; Bahn, R. C.; Griswold, J. J.; Schreiman, J. S. In: Jellins, J.; Kobayashi, T., eds. Evaluation of interpretation methods for transmission of the breast. Chichester: Wiley; 1983:211–221.

Greenleaf, J. F.; Johnson, S. A.; Lee, S. L.; Herman, G. T.; Wood, E. H. Algebraic reconstruction of spatial distributions of acoustic absorption within tissue from their two-dimensional acoustic projections. In: Green, P. S., ed. Acoustical holography 5. New York: Plenum Press; 1974:591–603.

Greenleaf, J. F.; Johnson, S. A.; Lent, A. H. Measurement of spatial distribution of refractive index in tissues by ultrasonic computed assisted tomography. Ultras. Med. Biol. 3:327–339; 1978.

Johnson, S. A.; Greenleaf, J. F.; Samayoa, W. F.; Duck, F. A.; Sjostrand, J. Reconstruction of three-dimensional velocity fields and other parameters by acoustic ray tracing. In: DeKlerk, J.; McAvoy, B. R., eds. IEEE ultras. symp. proc. New York: IEEE; 1975:46–51.

Kak, A. C.; Dines, K. A. Signal processing of broadband pulsed ultrasound: Measurement of attenuation of soft biological tissues. IEEE Trans. Biomed. Eng. BME-25:321–343; 1978.

Klepper, J. L.; Brandenberger, G. H.; Bussey, J. L.; Miller, J. G. Phase cancellation, reflection and refraction effects in quantitative ultrasonic attenuation tomography. In: DeKlerk, J.; McAvoy, B. R., eds. IEEE ultras. symp. proc. IEEE cat. no. 77CH1264-1SU. New York: IEEE; 1977:182–188.

Koch, R.; Whiting, J. F.; Price, D. C.; McCaffrey, J. F.; Kossoff, G.; Reeve, T. S. Ultrasound computed tomography instrumentation and human studies. In: Jellins, J.; Kobayashi, T., eds. Ultras. imaging of the breast. Chichester: Wiley; 1983:187–199.

Kossoff, G.; Fry, E. K.; Jellins, J. Average velocity of ultrasound in the human female breast. J. Acoust. Soc. Am. 53:1730–1736; 1973.

Lachenbruch, P. A. Discriminant analysis. New York: Hafner Press; 1975.

Lambert, P. A.; Carson, P. L.; Dick, D. E.; Oughton, T. V.; Kubitschek, J. E. Improvements in ultrasonic CT data acquisition and preprocessing. In: Proc. IEEE-EMBS Conf-frontiers of engineering in health care. IEEE Cat. #79-GH-14407; 1979.

McNeil, B. J.; Hanley, J. A. Statistical approaches to clinical predictions. New Engl. J. Med. May:1292–1294; 1981.

Meyer, C. R.; Chenevert, T. L.; Carson, P. L. A method for reducing multipath artifacts in ultrasonic computed tomography. JASA 72:820–824; 1982.

Mueller, R. D.; Kaveh, M.; Wade, G. Acoustic reconstructive tomography. Proc. IEEE 67:567–587; 1979.

Nie, N. H.; Hull, C. H.; Jenkins, C. G.; Steinbrenner, K.; Bent, D. H. Statistical package for the social sciences. New York: McGraw Hill; 1975.

Pan, K. M.; Liu, C. N. Tomographic reconstruction of ultrasonic attenuation with correction of refractive errors. IBM J. Res. Develop. 25:71–82; 1981.

Schmitt, R. M.; Meyer, C. R.; Carson, P. L.; Chenevert, T. L.; Bland, P. H. Error reduction in through transmission tomography using large receiving arrays with phase-insensitive signal processing. IEEE Trans. Sonics Ultrason. SU-31:251–258; 1984.

Schreiman, J. S.; Gisvold, J. J.; Greenleaf, J. F.; Bahn, R. C. Radiology 150:523–530; 1984.

Wolfe, J. N. Mammography. Illinois: Charles C. Thomas Publishers; 1967.